Metabolic rerouting by gain-of-function mutations overcomes *plsX* essentiality in *Staphylococcus aureus*

Paprapach Wongdontree[1], Milya Palmier[1], Vincent Leguillier[1], Karine Gloux[1], David Halpern[1], Jamila Anba-Mondoloni[1], Alexandra Gruss[1#]

[1] Université Paris-Saclay, INRAE, AgroParisTech, Micalis Institute, 78350, Jouy-en-Josas, France.

[#] For correspondence: alexandra.gruss@inrae.fr

Keywords : *Staphylococcus aureus,* fatty acid, FASII, phospholipid synthesis, *plsX* deletion suppressors, FabF, FadM, acyl-CoA thioesterase, acyl-ACP thioesterase, ACP-binding.

Short title: **Metabolic rerouting rescues PlsX deletion**

Abstract

Phospholipids are essential components of most bacterial membranes. The PlsX acyltransferase initiates phospholipid synthesis by reversibly converting acyl-ACP (ACP, acyl carrier protein) to acyl-PO_4, the first phospholipid precursor. PlsX is dispensable in some bacteria, as alternative functions assure acyl-PO_4 production. In contrast, PlsX is considered indispensable in *Staphylococcus aureus*, unless exogenous fatty acids (FA) are provided. Here we report that gain-of-function suppressors of Δ*pls*X enable *S. aureus* growth without FA addition. The suppressors map to either the FA synthesis (FASII) enzyme FabF, or to a putative acyl-CoA thioesterase/ACP binding protein, designated FadM. The Δ*plsX* suppressors alleviate accumulation of long chain acyl-ACP, and produce shorter chain membrane FAs than the parental strain. Unlike wild type *S. aureus*, which can adapt to FASII inhibitors, Δ*plsX* suppressors remain fully sensitive, indicating that PlsX reverse activity is not compensated. Importantly, an interdependency between FabF and FadM functions shown here suggests a more general role for FadM in facilitating FA release from FabF-FA-ACP intermediates. In summary, *S. aureus fabF* and *fadM* mutations promote enzymatic flexibility that overcomes Δ*pls*X growth arrest by restoring phospholipid synthesis.

Importance

Phospholipids are common and vital cell membrane components. Many bacteria initiate phospholipid synthesis using an enzyme called PlsX; some of them also have a backup system to ensure phospholipid synthesis and survival even if PlsX is disabled. However *Staphylococcus aureus*, a major pathogen, reportedly lacked a PlsX backup system. Here we used a genetic selection approach to show that *S. aureus* generates "gain-of-function" mutations, allowing bacteria to initiate phospholipid synthesis when PlsX is inactive. Bacteria survive thanks to a mutation in FabF, a fatty acid biosynthesis enzyme, or in FadM, a little-studied protein; our data indicate that FabF and FadM cooperate to compensate a PlsX defect. The outcome with either mutation is that bacteria produce and release fatty acids to patch into phospholipid synthesis. This study illustrates how new enzymatic circuitry is created by mutation to rescue bacteria from a potentially lethal membrane phospholipid synthesis defect.

Introduction

Lipids provide the essential scaffolding for cell membranes and life. Bacterial phospholipid membranes comprise fatty acids (FA) that are attached to a glycerophosphate backbone (1). The phospholipid FAs are either produced by the FA synthesis (FASII) pathway or captured from the environment (2). The acyl-Acyl Carrier Protein (acyl-ACP, or FA-ACP) intermediate is a substrate for three enzymes, involving FabF for FA elongation *via* FASII, and PlsX and PlsC for respectively the first and second steps of phospholipid synthesis (**Fig. 1**).

The membrane-associated acyltransferase PlsX is the first dedicated enzyme for phospholipid synthesis in Bacillota bacteria (3). It reversibly catalyzes conversion of acyl-ACP produced by FASII, to acyl-phosphate (acyl-PO_4), which is in turn used by membrane glycerol-3-phosphate acyltransferase PlsY to transfer the FA from acyl-PO_4 to the 1-position of the glycerophosphate backbone. Reversible PlsX activity produces acyl-ACP from acyl-PO_4, which allows bacteria to recover exogenous FAs (eFAs) after being phosphorylated by the FA kinase Fak (4, 5). The acyl-ACP may then re-enter the FASII system or be used by PlsC for phospholipid production (**Fig. 1**). PlsX reverse activity *via* the use of eFAs allows bacteria to overcome the need for FASII, such that they are insensitive to FASII inhibitors (6-8). In *Bacillus subtilis*, PlsX tethering to the membrane is required for phospholipid synthesis presumably to transfer its product to PlsY; however, this membrane association is not required for the reverse activity (9). PlsX is thus a sorting station that initiates phospholipid synthesis, or returns acyl groups for FASII elongation and PlsC processing.

Despite its pivotal role, PlsX is dispensable according to conditions and bacteria. Numerous bacteria among the Pseudomonadota encode PlsB, which has functional redundancy to PlsX-PlsY (3). In Bacillota, when eFAs are present, Fak-mediated phosphorylation produces the needed acyl-PO_4 substrate (4, 5). In the absence of FAs, some Bacillota pathogens deploy acyl-ACP thioesterases that liberate endogenous FAs from acyl-ACP**,** which may serve as Fak substrates to initiate phospholipid synthesis (10-13). Acyl-ACP thioesterase fully restores growth of *Streptococcus pneumoniae* Δ*plsX* (11), and conditionally rescues *Enterococcus faecalis* Δ*plsX* growth (the thioesterase preferentially cleaves acyl-ACP comprising unsaturated FAs, while growth is stimulated by saturated FAs; (12)). The presence of this alternative system may contribute to bacterial survival when PlsX function is impaired. A notable exception is the major human pathogen *Staphylococcus aureus*, which lacks an acyl-ACP thioesterase to liberate FAs. In this species, only eFAs or a cloned heterologous acyl-ACP thioesterase reportedly allowed growth of a *plsX* deletion strain (5).

Using positive genetic selections, we identified gain-of-function mutations that rescue Δ*plsX* viability. The Δ*plsX* suppressors map either to the FASII enzyme FabF, a 3-oxoacyl-ACP synthase II, or to a putative acyl-CoA thioesterase and ACP binding protein, designated as FadM. Our findings show that FadM and FabF cooperate to supply FAs when PlsX is defective, and suggest a role for FadM during wild type (WT) growth in regulating FASII metabolic flux.

Results and Discussion

Construction and confirmation of a Δ*plsX* in-frame mutant. *plsX* is the second gene in a multicistronic operon (**Fig. S1**). We constructed in-frame Δ*plsX* mutants of RN-R (RN4220 repaired for a defective *fakB1* gene in the 8325 lineage (14)) and of USA300_FPR3757 JE2 strains. Both Δ*plsX* mutants failed to grow on solid medium in the absence of FAs. Deletions were confirmed by full genome sequencing (**Table S2**) and by growth complementation in the absence of FAs using a plasmid-carried copy of the intact *plsX* gene (**Fig. S2;** shown in the RN-R background).

FA auxotrophy of *S. aureus* Δ*plsX* mutants is suppressed by mutations in *fabF*. During phenotypic characterization of the purified confirmed JE2 Δ*plsX* mutant, we noted the appearance of colonies on BHI medium without FA. Three colonies (designated Sup1, Sup2, and Sup3) were isolated and subjected to whole genome sequencing. In addition to the in-frame *plsX* deletion, point mutations were identified in the suppressors (**Table S1**; see **Table S2** for variant information). Mutations in Sup1 and Sup2 mapped to FabF (SAUSA300_0886), the 3-oxoacyl-ACP synthase II of the FASII elongation cycle (see **Fig. 1**), producing $FabF^{A119E}$ (alanine to glutamic acid; Sup1) and $FabF^{D266A}$ (aspartic acid to alanine; Sup2). However, the suppressor carrying $FabF^{D266A}$ was not recoverable from the primary stocked strain, possibly because the mutation was deleterious for growth. Sup1 and Sup2 also carried the same point mutation in *csa1A* (SAUSA300_0100), encoding a tandem lipoprotein. Sup3 carried a mutation in the SAUSA300_0150 gene, which is annotated as encoding a transposase that is not conserved among *S. aureus* strains, and was not further studied.

To further analyze Δ*plsX* suppression, we isolated 31 other suppressors from RN-R and JE2 backgrounds (16 and 15 suppressors, respectively), and screened for those carrying *fabF* mutations by PCR followed by DNA sequence analyses (**Table S1**, **Table S2**). Among them, 14

carried *fabF* mutations (12 in RN-R and 2 in JE2), which all mapped to the same *fabF* nucleotide position, resulting in a $FabF^{A119E}$ alteration as in Sup1. The DNA comprising *csa1A*, which carried a mutation in Sup1 and Sup2 mutants, was not mutated in the 14 *fabF* mutants. Since the same *fabF* mutation was found in both suppressor strain backgrounds, we conclude that this allele is responsible for the suppressor phenotype. This singular mutation could suggest that few FabF point modifications could allow both FASII activity and Δ*plsX* complementation.

We tried using plasmid complementation to directly show that the *fabF* mutation (called $fabF^m$) conferred Δ*plsX* suppression. A clone expressing $fabF^m$, but not WT *fabF* could be established in the WT RN-R strain by direct transformation; however, we failed to obtain the $fabF^m$ clone in the Δ*plsX* background, even in medium supplemented with FA. This suggested that *fabF* overexpression was toxic in *S. aureus*, consistent with reported *fabF* toxicity in *Escherichia coli* (15).

As an alternate approach, we used a FabF inhibitor, platensimycin, to determine whether disabling FabF was responsible for Δ*plsX* suppression. This antibiotic binds to the acyl-ACP-FabF intermediate, and competes with malonyl-ACP entry, thus preventing FA elongation (16). We reasoned that platensimycin addition might mimic the FabF suppressor mutation, and could be used to test whether the mutated *fabF* allele is the direct Δ*plsX* suppressor. Cultures of Δ*plsX* (RN-R strain background) were grown in liquid medium containing C18:1, and then washed and resuspended in BHI medium without FAs. Bacterial dilutions were plated on BHI solid medium, and platensimycin (1.5 µg) was spotted in the center of plates, which were incubated at 37°C for 96 h and photographed (**Fig. 2**). In addition to the emergence of Δ*plsX* suppressors, a distinct homogeneous growth ring was observed around the platensimycin spots. Since the *fabF* mutants and a FabF inhibitor both restore Δ*plsX* growth, we consider it likely that the FabF mutation is directly responsible for Δ*plsX* suppression.

FA auxotrophy of *S. aureus* Δ*plsX* mutants is suppressed by mutations in *fadM*. As 17 suppressors isolated above carried a wild-type (WT) *fabF* sequence, we searched for mutations elsewhere that conferred growth on BHI. Three isolates not mutated in *fabF* were randomly selected among the Δ*plsX* suppressors for genomic DNA sequencing, one derived from RN-R Δ*plsX* and two from JE2 Δ*plsX* backgrounds. A single common gene target, SAOUHSC_01348 in RN-R or SAUSA300_1247 in JE2, was mutated in all sequenced suppressors (**Table S1**). The 155-amino-acid Orf shares ~20% identity and ~40% similarity to the *E. coli* acyl-CoA thioesterase FadM (PBD database protein 6FDG_A), with a conserved catalytic triad (17, 18); we refer here to the *S. aureus* Orf as FadM. FadM reportedly has a dual function in both *E. coli* and *S. aureus*,

as an acyl-CoA thioesterase and an ACP-binding protein (17, 19-21). The *S. aureus fadM* gene was PCR-amplified and sequenced in all the other suppressors lacking mutations in *fabF*. All 17 of them carried mutations in *fadM*. A single variant (encoding FadM^{Y90F}, [*fadM*^{m2}]) was identified in the four isolates selected from RN-R Δ*plsX*; three distinct FadM variants were identified among the JE2 Δ*plsX* suppressors (FadM^{I38T} [*fadM*^{m1}], FadM^{Y90F} [*fadM*^{m2}], and FadM^{Y133F} [*fadM*^{m3}]) (**Table S1**, **Table S2**). As all identified mutations mapped to either *fabF* or *fadM*, we conclude that FabF and FadM are the main mutational suppressors able to rescue Δ*plsX* growth.

Although *E. coli* expresses both PlsX-PlsY, and the functionally redundant enzyme PlsB (3), Δ*plsX*Δ*plsY* is synthetically lethal (22). Suppressors of *E. coli* Δ*plsX*Δ*plsY* lethality displayed increased pools of glycerol-3-phosphate (Gly-3-P), the backbone for FA attachment to produce phospholipids (22). Increased Gly-3-P presumably compensates low efficiency acyl-transferase activity of PlsB compared to PlsY. Remarkably, the *E. coli* (22) and *S. aureus* (this study) selections yielded no common suppressors. This may reflect the functional divergence between these species, and/or the use of a single non-redundant target, PlsX, for *S. aureus* selections.

FadM inactivation abolishes Δ*plsX* suppression. *fadM* is the downstream gene in a 2-gene operon also comprising *acnA* ((23); **Fig. S1**). To confirm that *fadM* is responsible for the Δ*plsX* suppressor phenotype, we inactivated the gene by transducing a *fadM* transposon insertion from the NARSA library into the JE2 Δ*plsX fadM*^{m2} suppressor (strain 7.1; **Table S1**), giving rise to Δ*plsX fadM*::Tn, and selecting with 5 µg/ml erythromycin (24). Insertion was confirmed by PCR. The Δ*plsX fadM*::Tn strain failed to grow on FA-free medium (**Fig. 3**). We conclude that Δ*plsX* growth relies on FadM mutant activity, and not its inactivation.

Evidence that FadM ACP binding, and not thioesterase activity is involved in FadM mutant–mediated suppression. We asked which of the two potential FadM functions, acyl-CoA thioesterase or ACP binding, could be important for Δ*plsX* suppression. A recent structure-function study of *S. aureus* FadM mapped key amino acids of the acyl-binding cavity, which presents the acyl-CoA substrate for thioesterase cleavage (17). Notably, FadM suppressor mutations coincide or are adjacent to the amino acids within the cavity, as based on FadM crystal structure (PDB: 6FDG, and Alphafold design (https://alphafold.ebi.ac.uk/entry/A0A0H2XFE3) (**Fig. S3A**). The grouped location of mutations within the acyl-binding cavity needed for thioesterase activity suggests that this function is defective in the FadM suppressor mutants.

We further ruled out a positive role for acyl-CoA thioesterase in Δ*plsX* suppression. The

FadM thioesterase substrate is acyl-CoA, which is synthesized by acyl-CoA synthetase, annotated as FadE in *S. aureus* (25, 26). If FadM acyl-CoA thioesterase were needed for Δ*plsX* suppression, acyl-CoA would first have to be produced by FadE, and then re-hydrolyzed by FadM, a futile cycle. The *fad* genes are subject to CcpA-mediated glucose repression (24, 26). Thus, if FadM thioesterase and FadE activity mediated Δ*plsX* suppression, suppression would be repressed by glucose, due to lower production of acyl-CoA. However, glucose did not affect suppressor phenotypes (**Fig. S3**). Since total loss of FadM does not promote Δ*plsX* suppression (**Fig. 3**), these observations show that FadM is required for Δ*plsX* suppression, but not through its acyl-CoA thioesterase activity. In view of the two known FadM activities, we conclude that ACP binding is the FadM activity mediating *S. aureus* Δ*plsX* suppression.

Impact of Δ*plsX* suppressors on bacterial growth. We assessed growth of Δ*plsX* suppressors in RN-R and JE2 backgrounds in non-FA-supplemented BHI medium (**Fig. 4**). The initial Δ*plsX* deletion strains fail to grow unless supplemented with FAs. The *fabF* and *fadM* suppressor mutants grew similarly, but their growth phenotypes differed between the parental strains: in the RN-R background, growth of both tested suppressors was intermediate between the WT strain and the Δ*plsX* mutant. In contrast, all suppressors grew essentially as the WT in the JE2 background. A distinguishing feature between the two *S. aureus* strains is the production of staphyloxanthin pigment by JE2 but not by RN-R (an RN4220 derivative). As staphyloxanthin comprises an acyl moiety (27), its production in JE2 and suppressor strains might improve membrane integrity. This hypothesis remains to be tested.

Impact of Δ*plsX* suppressors on membrane FA composition. We assessed membrane FA composition of Δ*plsX* suppressors in RN-R and JE2 backgrounds in medium devoid of FAs (**Fig. 5**). The *fabF* suppressor strains produced membrane FAs of shorter overall length in both strain backgrounds; *ai*17 (anteiso17) is the longest main FA in those profiles. Notably, the straight-chain FAs C18:0 and C20:0, are present in parental strains but absent in *fabF* suppressors. This could be explained if the mutated $FabF^{A119E}$ suppressor allele is partially defective for elongating the acyl-ACP substrate. In *S. aureus*, branched chain precursors are preferred substrates for FabH (see **Fig. 1**; (28)), which could explain the presence of only branched chain FAs in $fabF^{m}$ strains. FA profiles in $fadM^{m}$ suppressor strains were more similar to parental profiles, but like the *fabF* suppressor, produced proportionately less C18:0 and C20:0.

Acyl-ACP distribution in JE2 WT, Δ*plsX*, and Δ*plsX* suppressors. Blocking the first step of phospholipid synthesis by *plsX* deletion results in accumulation of acyl-ACP (5, 29). This intermediate cannot be used by PlsC to produce phosphatidic acid until position 1 of the glycerophosphate backbone is occupied, a reaction that is not assured in the Δ*plsX* strain (**Fig. 1**; (5)). We assessed acyl-ACP intermediate accumulation in the Δ*plsX* mutant and Δ*plsX* suppressors by submitting samples to polyacrylamide gel electrophoresis run in non-denaturing conditions, and hybridizing with anti-ACP antibodies (7, 30) (**Fig. 6**). Unlike the WT strain, the Δ*plsX* mutant was distinguished by the presence of a fast-migrating band corresponding to ACP bound to long-chain FAs. In contrast, the long acyl-ACP species was absent in both Δ*plsX fabF*^{m} and Δ*plsX fadM*^{m} suppressors, indicating that acyl-ACP is processed to initiate phospholipid synthesis, and in keeping with the good growth of suppressors. We propose that FabF or FadM mutations increase availability of free FAs, which are phosphorylated by Fak and then transferred to position 1 of the glycerophosphate backbone. PlsC then uses the accumulated acyl-ACP to produce phosphatidic acid, thus alleviating the roadblock (**Fig. 1**).

Δ*plsX* suppressors do not restore reverse PlsX activity, which is required to bypass the FASII pathway. We asked whether *fabF* and/or *fadM* suppressor strains also complemented the reverse PlsX activity, i.e., formation of acyl-ACP from acyl-PO_4 (**Fig. 1**). If this were the case, FASII inhibition would be overcome by addition of eFAs to medium. To test this, WT strain JE2, and isogenic Δ*plsX*, Δ*plsX fabF*^{m}, and Δ*plsX fadM*^{m} strains were grown in medium containing FAs (SerFA), without and with the FASII inhibitor AFN-1252 (31) (**Fig. 7**). All strains grew to equivalent densities in the absence of anti-FASII. The JE2 WT strain overcame the presence of AFN-1252 when FAs were supplied (6, 8). In contrast, neither the Δ*plsX* mutant nor the Δ*plsX* suppressors could overcome FASII inhibition. These findings prove that the reverse reaction catalyzed by PlsX is not compensated by *fabF* or *fadM* suppressor mutations, and that an active FASII pathway is required for suppressor growth. They also show that the PlsX reverse reaction is required for FASII bypass.

Evidence that FabF and FadM mutations contribute to the same suppressor pathway. We showed that *fadM* interruption in the Δ*plsX fadM*^{m2} suppressor strain (giving rise to Δ*plsX fadM*::Tn) abolished the suppressor effect (**Fig. 3**). As the Tn insertion eliminated *fadM* as a potential target, we reasoned that any further suppressors would map to *fabF*. This hypothesis was tested by plating the JE2 Δ*plsX fadM*::Tn mutant on BHI medium in the same conditions as used to obtain suppressors (**Table S1** and **Materials and Methods**). Unexpectedly, no

suppressors arose after extended (> 1 week) plate incubation at 37°C compared to frequent mutant emergence in the Δ*plsX* background after 1-2 days (**Fig. 8A**). These results indicate that intact FadM, whether wild type or mutated, is required to obtain FabF suppression of Δ*plsX*.

The implication of FadM in FabF suppression was further tested by comparing the effects of platensimycin, the FabF inhibitor, in the Δ*plsX* and Δ*plsX fadM*::Tn backgrounds. Compared to the Δ*plsX* mutant, the Δ*plsX fadM*::Tn mutant appeared to be more platensimycin-sensitive, and did not produce a visible growth ring compared to the Δ*plsX* strain (**Fig. 8B**). These results affirm that FadM is required for Δ*plsX* suppression *via* FabF. We conclude that FabF and FadM interact in the same pathway.

Conclusions

This study shows that PlsX, which is reportedly required for *S. aureus* growth in the absence of eFAs, can be compensated by gain-of-function mutations in either FabF or in a little-characterized bi-functional protein, FadM, with reported acyl-CoA thioesterase and ACP binding activity (17, 20). Here we identified a previously unknown cooperative link between FabF and FadM, and adds FadM among the factors implicated in *S. aureus* phospholipid metabolism. We propose a model in which FadM facilitates ACP removal from the acyl-ACP-FabF intermediate, prior to malonyl-ACP entry (32) (**Fig. 9**): the $FabF^{A119E}$ mutant rescues Δ*plsX* by releasing its FA cargo just before malonyl-ACP entry. By binding ACP, FadM may facilitate ACP removal from the FabF cavity, thus favoring FA liberation for its phosphorylation, and subsequent phospholipid synthesis initiation. We speculate that the FadM suppressor mutations are defective for acyl-CoA thioesterase activity due to mutations affecting the FA cavity (**Fig. S3**), which would leave more FadM available for ACP binding to the FabF intermediate. Thus, either FabF mutation, or more efficient FadM-mediated removal of ACP from the FabF-acyl-ACP intermediate, would increase FA release by FabF. Total loss of FadM would reduce free FA release from the FabF ping-pong intermediates, explaining the lack of suppressors in the Δ*plsX fadM*::Tn background (**Fig. 8**). It remains to be determined whether FadM contributes to FASII homeostasis during normal WT growth. FadM could act as an FA release valve that decreases FabF processivity to modulate phospholipid chain length. Altogether, these findings identify another actor involved in the FASII pathway, and show how metabolic rewiring may occur by simple point mutations in response to a selective pressure.

Materials and methods

Strains, growth conditions, and plasmids. Strains and plasmids are listed in **Table S3**. *S. aureus* strains are derived from USA300_FPR3757 strain JE2 (24) and RN4220-R (called here RN-R; (14)). RN-R is a readily transformable strain derived from RN4220, of the NCTC 8325 lineage (33). It was repaired to restore a functional *fakB1* gene, which is defective in the entire NCTC 8325 lineage (14)). *S. aureus* cultures were grown at 37°C with shaking unless otherwise specified. The Δ*plsX* mutants were grown on BHI medium containing C18:1 fatty acid at a concentration of 250 µM (Larodan, Sweden), unless otherwise specified. Parental strains and Δ*plsX*-suppressor mutants were grown in BHI medium (Brain Heart Infusion; Gibco, France) at 37°C with shaking. The FabI inhibitor AFN-1252 (Med ChemExpress, France) and FabF inhibitor platensimycin (Bioaustralis-Tebubio France) were used as specified (16, 34).

***plsX* mutant construction.** The Δ*plsX* mutants were constructed in RN-R (RN4220 repaired for a defective *fakB1* gene in the NCTC8325 lineage; (14)) and JE2 backgrounds. The preparatory plasmid for *plsX* deletion was constructed using the Gibson assembly method to insert DNA segments flanking the *plsX orf* into Sma1-linearized pMAD, a thermosensitive plasmid expressing erythromycin resistance (35, 36). Oligonucleotides for Δ*plsX* construction are in **Table S4**. Constructions were verified by DNA sequencing of PCR-amplified fragments. The double cross-over gene replacements were obtained as described (14, 36) in RN-R and JE2 strains. Deletions removed nucleotides 1,228,616-1,229,594 in JE2, and 1,148,670-1,149,648 in RN-R, as per respective annotated genomes. The resultant strain genotypes were confirmed by whole genome sequencing (Eurofins, Germany).

Cloning and complementation of the Δ*plsX* mutant in RN-R and JE2 strains. To confirm that strain characteristics were due to the *plsX* deletion, the intact *plsX* gene was cloned with its natural promoter (upstream of *fapR*) on multicopy plasmid pIM-locus1 (a pIMAY derivative (37, 38)). Cloning was performed by Gibson assembly with oligonucleotide primers (**Table S4**).

Isolation of suppressor mutants. RN-R Δ*plsX* and JE2 Δ*plsX* strains were first streaked on solid BHI medium containing 250 µM C18:1, an FA that promotes growth. For each strain, a single colony was used to inoculate a liquid culture (in BHI+C18:1). When the culture reached exponential phase, bacteria were centrifuged, resuspended in BHI, and adjusted to OD_{600} = 0.1. Dilutions were plated on solid medium to obtain ~10^5 to ~10^7 colony forming units per plate on solid BHI medium without FAs. Colonies were scored after two or more days of incubation at 37°C, and selected at random for restreaking on solid BHI medium. Liquid cultures were

prepared in BHI, and stocked in 20% glycerol for storage at -70°C. The stored mutant clones were analyzed by DNA sequencing to identify mutated loci.

Genomic DNA preparation for whole genome sequencing. Bacterial cell pellets, prepared from 3 mL liquid exponential phase cultures, were centrifuged at 8,000 rpm for 5 min. Pellets were re-suspended in 800 µL TE buffer (10 mM Tris- HC1, pH 8.0/1 mM EDTA) plus 20 µL lysostaphin 5 mg/mL, and incubated for 45 min at 37°C. DNA was prepared by DNeasy Blood & Tissue Kit (Qiagen, France) and samples were outsourced for whole genome DNA sequencing using 2x150 bp paired end chemistry and bioinformatics analyses (Eurofins Genomics, France) (6). SNPs that differed in non-antibiotic-treated JE2 and RN-R strains from those in the reference sequence (GenBank Nucleotide accession codes NC_007793.1 and NC_007795.1 respectively) were subtracted prior to variant identification. Variants were identified as representing ≥80% of reads in sequences for which there were at least 100 reads.

PCR amplification and confirmation by DNA sequencing. Selected candidate colonies were suspended in 100 µL of 0.9% NaCl with 1 µL of lysostaphin from a 5 mg/mL stock. Tubes containing suspensions were shaken for 45 min at 37°C. Contents were then transferred to tubes containing glass beads and samples were vortexed for 1 min. PCR amplification was performed using primers (**Table S4**) and Phusion DNA polymerase (ThermoFisher Scientific, France) according to manufacturer protocol, using a SimpliAmp Thermal Cycler (ThermoFisher Scientific, France). PCR products were analyzed on a 0.8% agarose gel prepared in 0.5% Tris acetate EDTA buffer (Euromedex) containing 0.5 µg/mL ethidium bromide. Gels were run at 100 V for 30 min in an electrophoresis chamber (Mupid ONE; Dutscher, France), and photographed under UV light using the EBOX VX5 imaging system (Vilber Lourmat, France). PCR samples were purified using the NucleoSpin® Gel and PCR Clean-up kit (Macherey-Nagel, France), and sent for DNA sequencing (Eurofins, France).

Effects of the FabF inhibitor platensimycin on Δ*plsX* and Δ*plsX fadM*::Tn strains. Strains were grown in BHI containing C18:1 (250 µM) overnight, washed once in BHI medium, and resuspended in BHI to a final density of OD_{600} = 0.1. From this, 100 µl of the bacterial suspension was plated on solid BHI medium. Platensimycin (1.5 µg in 3 µl) was spotted in the center of plates, which were then incubated at 37°C for 4-7 days and photographed.

Effect of glucose on growth of Δ*plsX* suppressors. Strains were precultured in liquid LB (n.b., LB lacks glucose) or LB with C18:1 for Δ*plsX* at 37°C. After overnight growth, cultures were diluted to OD_{600} = 0.05 and grown for 3-4 hours. Δ*plsX* cultures were first centrifuged and resuspended in fresh LB medium to remove free FAs present in medium. Bacterial densities were then

adjusted to OD_{600} = 1. Cultures were streaked on solid medium, corresponding to LB or LB containing 0.5% glucose, which represses *fad* operon expression (23, 26). Plates were incubated at 37°C for 24 hours and photographed.

Growth kinetics. Three mL precultures were prepared in BHI for parental and Δ*plsX* suppressor strains, or in BHI containing 250 µM C18:1 for Δ*plsX* mutants. After overnight growth, culture OD_{600} were adjusted to OD_{600} = 0.05 in 200 µL BHI medium without or with C18:1 (250 µM), in 96-well microtiter plates. Growth was followed on a Spark M10 plate reader (Tecan, France). For experiments in which samples were taken for FA determinations or for Western blot experiments, cultures were prepared in 3 to 10 ml liquid cultures, and were monitored manually by OD_{600} measurements every two hours.

Determination of membrane FA profiles. Bacterial cultures (equivalent of OD_{600} = 2) were centrifuged, and pellets were washed once in 1 ml of 0.02% Triton in 0.9% NaCl, then twice with 1 ml of 0.9% NaCl. FA extractions were performed as described (6).

Detection of ACP products. Pellets from OD_{600}=10 equivalent of exponential phase cultures were collected by centrifugation (8000 rpm for 5 min), and then washed twice with PBS (Phosphate Buffer Saline)-Triton X100 0.1%, and once with PBS. Pellets were re-suspended in 600 µL PBS supplemented with 6 µL antiprotease (100X), 50 µg/mL lysostaphin and 50 µg/mL DNAse and incubated with shaking for 25 min at 37°C. Protein concentrations were determined (39). Protein extracts (10 µg) were loaded onto non-denaturing gels containing 1M urea and 14% acrylamide gel as described (5, 7). The separated proteins were transferred to a PVDF membrane (Biorad, France) by electroblotting using a current of 25 V and 1.3 A on a power blotter semi-dry transfer system (Invitrogen, France) for 7 min. The primary anti-ACP antibody (Covalabs, France; (7)) was used at 1:500 dilution and secondary anti-rabbit IgG conjugated with peroxidase (Invitrogen, France) at a 1:5000 dilution. ACP-reactive bands were identified using the ECL kit (Perkin Elmer, France) and the fluorescent signal was recorded using ChemiDoc (BioRad, France). Analysis was done by the Image Lab 5.0 program.

Phage transduction. Transduction of transposon insertions from JE2 into Δ*plsX* mutant backgrounds was performed as described (40) using ϕ80 phage stock.

FASII bypass of WT and Δ*plsX* derivative strains. Strains were grown overnight in liquid SerFA medium (SerFA, BHI containing 10 % newborn calf serum and an equimolar mixture of 85 µM each C14:0, C16:0, and C18:1 [Larodan, Sweden]). Cultures were then diluted to OD_{600}=0.05 in SerFA containing or not the anti-FASII AFN-1252 (here called AFN; (31); MedChemExpress, France). Growth was monitored using the Spark plate reader (Tecan, France).

Acknowledgements and funding

We are grateful to Kam Pou Han and Philippe Bouloc (Bouloc lab, I2BC, Orsay, France) for providing transducing phage and plasmid; Florence Dubois-Brissonet and Katia de Oliveira (Micalis, INRAE) for their expert help and advice with CpG analyses; Olivier Son for help with phage transduction materials. We thank Micalis Institute colleagues Vincent Juillard for discussion of PlsX functions, Clara Louche for critical reading of the manuscript, and Philippe Gaudu for stimulating discussion.

This work was supported by the French Agence Nationale de la Recherche ANR (ANR-16-CE15-0013; AG), the Joint Programming Initiative on Antimicrobial Resistance (JPIAMR) under the umbrella of the ANR (ANR-22-AAMR-0007; AG), and the Fondation pour la Recherche Medicale (DBF20161136769; AG).

Data availability

All relevant data are within the manuscript, supporting information files, and repositories. Any biological materials are available upon request.

Author Contributions

All authors performed, analyzed, and interpreted experiments, and approved the manuscript. PW, JAM, and AG conceived the project, designed research, and wrote the paper.

Competing interests

The authors declare no competing interests.

References

1. Zhang YM, Rock CO. 2008. Membrane lipid homeostasis in bacteria. Nat Rev Microbiol 6:222-33.
2. Silbert DF, Ruch F, Vagelos PR. 1968. Fatty acid replacements in a fatty acid auxotroph of *Escherichia coli*. J Bacteriol 95:1658-65.
3. Lu YJ, Zhang YM, Grimes KD, Qi J, Lee RE, Rock CO. 2006. Acyl-phosphates initiate membrane phospholipid synthesis in Gram-positive pathogens. Mol Cell 23:765-72.
4. Parsons JB, Broussard TC, Bose JL, Rosch JW, Jackson P, Subramanian C, Rock CO. 2014. Identification of a two-component fatty acid kinase responsible for host fatty acid incorporation by *Staphylococcus aureus*. Proc Natl Acad Sci U S A 111:10532-7.
5. Parsons JB, Frank MW, Jackson P, Subramanian C, Rock CO. 2014. Incorporation of extracellular fatty acids by a fatty acid kinase-dependent pathway in *Staphylococcus aureus*. Mol Microbiol 92:234-45.
6. Kenanian G, Morvan C, Weckel A, Pathania A, Anba-Mondoloni J, Halpern D, Gaillard M, Solgadi A, Dupont L, Henry C, Poyart C, Fouet A, Lamberet G, Gloux K, Gruss A. 2019. Permissive Fatty Acid Incorporation Promotes Staphylococcal Adaptation to FASII Antibiotics in Host Environments. Cell Rep 29:3974-3982 e4.
7. Morvan C, Halpern D, Kenanian G, Hays C, Anba-Mondoloni J, Brinster S, Kennedy S, Trieu-Cuot P, Poyart C, Lamberet G, Gloux K, Gruss A. 2016. Environmental fatty acids enable emergence of infectious *Staphylococcus aureus* resistant to FASII-targeted antimicrobials. Nat Commun 7:12944.
8. Wongdontree P, Millan-Oropeza A, Upfold J, Lavergne JP, Halpern D, Lambert C, Page A, Kenanian G, Grangeasse C, Henry C, Fouet A, Gloux K, Anba-Mondoloni J, Gruss A. 2024. Oxidative stress is intrinsic to staphylococcal adaptation to fatty acid synthesis antibiotics. iScience 27:109505.
9. Sastre DE, Pulschen AA, Basso LGM, Benites Pariente JS, Marques Netto CGC, Machinandiarena F, Albanesi D, Navarro M, de Mendoza D, Gueiros-Filho FJ. 2020. The phosphatidic acid pathway enzyme PlsX plays both catalytic and channeling roles in bacterial phospholipid synthesis. J Biol Chem 295:2148-2159.
10. Jing F, Cantu DC, Tvaruzkova J, Chipman JP, Nikolau BJ, Yandeau-Nelson MD, Reilly PJ. 2011. Phylogenetic and experimental characterization of an acyl-ACP thioesterase family reveals significant diversity in enzymatic specificity and activity. BMC Biochem 12:44.
11. Parsons JB, Frank MW, Eleveld MJ, Schalkwijk J, Broussard TC, de Jonge MI, Rock CO. 2015. A thioesterase bypasses the requirement for exogenous fatty acids in the *plsX* deletion of *Streptococcus pneumoniae*. Mol Microbiol 96:28-41.
12. Zou Q, Dong H, Cronan JE. 2023. Growth of *Enterococcus faecalis* Δ*plsX* strains is restored by increased saturated fatty acid synthesis. mSphere 8:e0012023.
13. Cross B, Garcia A, Faustoferri R, Quivey RG. 2016. PlsX deletion impacts fatty acid synthesis and acid adaptation in *Streptococcus mutans*. Microbiology (Reading) 162:662-671.
14. Pathania A, Anba-Mondoloni J, Gominet M, Halpern D, Dairou J, Dupont L, Lamberet G, Trieu-Cuot P, Gloux K, Gruss A. 2021. (p)ppGpp/GTP and Malonyl-CoA Modulate *Staphylococcus aureus* Adaptation to FASII Antibiotics and Provide a Basis for Synergistic Bi-Therapy. mBio 12.
15. Subrahmanyam S, Cronan JE, Jr. 1998. Overproduction of a functional fatty acid biosynthetic enzyme blocks fatty acid synthesis in *Escherichia coli*. J Bacteriol 180:4596-602.
16. Wang J, Soisson SM, Young K, Shoop W, Kodali S, Galgoci A, Painter R, Parthasarathy G, Tang YS, Cummings R, Ha S, Dorso K, Motyl M, Jayasuriya H, Ondeyka J, Herath K, Zhang C, Hernandez L, Allocco J, Basilio A, Tormo JR, Genilloud O, Vicente F, Pelaez F, Colwell L, Lee SH, Michael B, Felcetto T, Gill C, Silver LL, Hermes JD, Bartizal K, Barrett J, Schmatz D, Becker JW, Cully D, Singh SB. 2006. Platensimycin is a selective FabF inhibitor with potent antibiotic properties. Nature 441:358-61.

17. Murad AM, Brognaro H, Falke S, Lindner J, Perbandt M, Mudogo C, Schubert R, Wrenger C, Betzel C. 2022. Structure and activity of the DHNA Coenzyme-A Thioesterase from *Staphylococcus aureus* providing insights for innovative drug development. Sci Rep 12:4313.
18. Swarbrick CMD, Nanson JD, Patterson EI, Forwood JK. 2020. Structure, function, and regulation of thioesterases. Prog Lipid Res 79:101036.
19. Butland G, Peregrin-Alvarez JM, Li J, Yang W, Yang X, Canadien V, Starostine A, Richards D, Beattie B, Krogan N, Davey M, Parkinson J, Greenblatt J, Emili A. 2005. Interaction network containing conserved and essential protein complexes in *Escherichia coli*. Nature 433:531-7.
20. Cherkasov A, Hsing M, Zoraghi R, Foster LJ, See RH, Stoynov N, Jiang J, Kaur S, Lian T, Jackson L, Gong H, Swayze R, Amandoron E, Hormozdiari F, Dao P, Sahinalp C, Santos-Filho O, Axerio-Cilies P, Byler K, McMaster WR, Brunham RC, Finlay BB, Reiner NE. 2011. Mapping the protein interaction network in methicillin-resistant *Staphylococcus aureus*. J Proteome Res 10:1139-50.
21. Gully D, Bouveret E. 2006. A protein network for phospholipid synthesis uncovered by a variant of the tandem affinity purification method in *Escherichia coli*. Proteomics 6:282-93.
22. Rex AN, Simpson BW, Bokinsky G, Trent MS. 2024. PlsX and PlsY: Additional roles beyond glycerophospholipid synthesis in Gram-negative bacteria. mBio doi:10.1128/mbio.02969-24:e0296924.
23. Mader U, Nicolas P, Depke M, Pane-Farre J, Debarbouille M, van der Kooi-Pol MM, Guerin C, Derozier S, Hiron A, Jarmer H, Leduc A, Michalik S, Reilman E, Schaffer M, Schmidt F, Bessieres P, Noirot P, Hecker M, Msadek T, Volker U, van Dijl JM. 2016. *Staphylococcus aureus* Transcriptome Architecture: From Laboratory to Infection-Mimicking Conditions. PLoS Genet 12:e1005962.
24. Fey PD, Endres JL, Yajjala VK, Widhelm TJ, Boissy RJ, Bose JL, Bayles KW. 2013. A genetic resource for rapid and comprehensive phenotype screening of nonessential *Staphylococcus aureus* genes. MBio 4:e00537-12.
25. Fujita Y, Matsuoka H, Hirooka K. 2007. Regulation of fatty acid metabolism in bacteria. Mol Microbiol 66:829-39.
26. Kuiack RC, Tuffs SW, Dufresne K, Flick R, McCormick JK, McGavin MJ. 2023. The *fadXDEBA* locus of *Staphylococcus aureus* is required for metabolism of exogenous palmitic acid and in vivo growth. Mol Microbiol 120:425-438.
27. Pelz A, Wieland KP, Putzbach K, Hentschel P, Albert K, Gotz F. 2005. Structure and biosynthesis of staphyloxanthin from *Staphylococcus aureus*. J Biol Chem 280:32493-8.
28. Qiu X, Choudhry AE, Janson CA, Grooms M, Daines RA, Lonsdale JT, Khandekar SS. 2005. Crystal structure and substrate specificity of the beta-ketoacyl-acyl carrier protein synthase III (FabH) from *Staphylococcus aureus*. Protein Sci 14:2087-94.
29. Machinandiarena F, Nakamatsu L, Schujman GE, de Mendoza D, Albanesi D. 2020. Revisiting the coupling of fatty acid to phospholipid synthesis in bacteria with FapR regulation. Mol Microbiol 114:653-663.
30. Cronan JE, Thomas J. 2009. Bacterial fatty acid synthesis and its relationships with polyketide synthetic pathways. Methods Enzymol 459:395-433.
31. Karlowsky JA, Kaplan N, Hafkin B, Hoban DJ, Zhanel GG. 2009. AFN-1252, a FabI inhibitor, demonstrates a Staphylococcus-specific spectrum of activity. Antimicrob Agents Chemother 53:3544-8.
32. Mindrebo JT, Patel A, Kim WE, Davis TD, Chen A, Bartholow TG, La Clair JJ, McCammon JA, Noel JP, Burkart MD. 2020. Gating mechanism of elongating beta-ketoacyl-ACP synthases. Nat Commun 11:1727.
33. Herbert S, Ziebandt AK, Ohlsen K, Schafer T, Hecker M, Albrecht D, Novick R, Gotz F. 2010. Repair of global regulators in *Staphylococcus aureus* 8325 and comparative analysis with other clinical isolates. Infect Immun 78:2877-89.
34. Hunt T, Kaplan N, Hafkin B. 2016. Safety, tolerability and pharmacokinetics of multiple oral doses

of AFN-1252 administered as immediate release (IR) tablets in healthy subjects. J Chemother 28:164-71.
35. Arnaud M, Chastanet A, Debarbouille M. 2004. New vector for efficient allelic replacement in naturally nontransformable, low-GC-content, gram-positive bacteria. Appl Environ Microbiol 70:6887-91.
36. Biswas I, Gruss A, Ehrlich SD, Maguin E. 1993. High-efficiency gene inactivation and replacement system for gram-positive bacteria. J Bacteriol 175:3628-35.
37. Coronel-Tellez RH, Pospiech M, Barrault M, Liu W, Bordeau V, Vasnier C, Felden B, Sargueil B, Bouloc P. 2022. sRNA-controlled iron sparing response in Staphylococci. Nucleic Acids Res 50:8529-8546.
38. Monk IR, Shah IM, Xu M, Tan MW, Foster TJ. 2012. Transforming the untransformable: application of direct transformation to manipulate genetically *Staphylococcus aureus* and *Staphylococcus epidermidis*. mBio 3.
39. Bradford MM. 1976. A rapid and sensitive method for the quantitation of microgram quantities of protein utilizing the principle of protein-dye binding. Anal Biochem 72:248-54.
40. Bowring JZ, Su Y, Alsaadi A, Svenningsen SL, Parkhill J, Ingmer H. 2022. Screening for Highly Transduced Genes in *Staphylococcus aureus* Revealed Both Lateral and Specialized Transduction. Microbiol Spectr 10:e0242321.
41. Brown ED. 2006. Microbiology: antibiotic stops 'ping-pong' match. Nature 441:293-4.
42. Jumper J, Evans R, Pritzel A, Green T, Figurnov M, Ronneberger O, Tunyasuvunakool K, Bates R, Zidek A, Potapenko A, Bridgland A, Meyer C, Kohl SAA, Ballard AJ, Cowie A, Romera-Paredes B, Nikolov S, Jain R, Adler J, Back T, Petersen S, Reiman D, Clancy E, Zielinski M, Steinegger M, Pacholska M, Berghammer T, Bodenstein S, Silver D, Vinyals O, Senior AW, Kavukcuoglu K, Kohli P, Hassabis D. 2021. Highly accurate protein structure prediction with AlphaFold. Nature 596:583-589.
43. Varadi M, Bertoni D, Magana P, Paramval U, Pidruchna I, Radhakrishnan M, Tsenkov M, Nair S, Mirdita M, Yeo J, Kovalevskiy O, Tunyasuvunakool K, Laydon A, Zidek A, Tomlinson H, Hariharan D, Abrahamson J, Green T, Jumper J, Birney E, Steinegger M, Hassabis D, Velankar S. 2024. AlphaFold Protein Structure Database in 2024: providing structure coverage for over 214 million protein sequences. Nucleic Acids Res 52:D368-D375.
44. Monk IR, Stinear TP. 2021. From cloning to mutant in 5 days: rapid allelic exchange in *Staphylococcus aureus*. Access Microbiol 3:000193.
45. Christie GE, Matthews AM, King DG, Lane KD, Olivarez NP, Tallent SM, Gill SR, Novick RP. 2010. The complete genomes of *Staphylococcus aureus* bacteriophages 80 and 80alpha--implications for the specificity of SaPI mobilization. Virology 407:381-90.

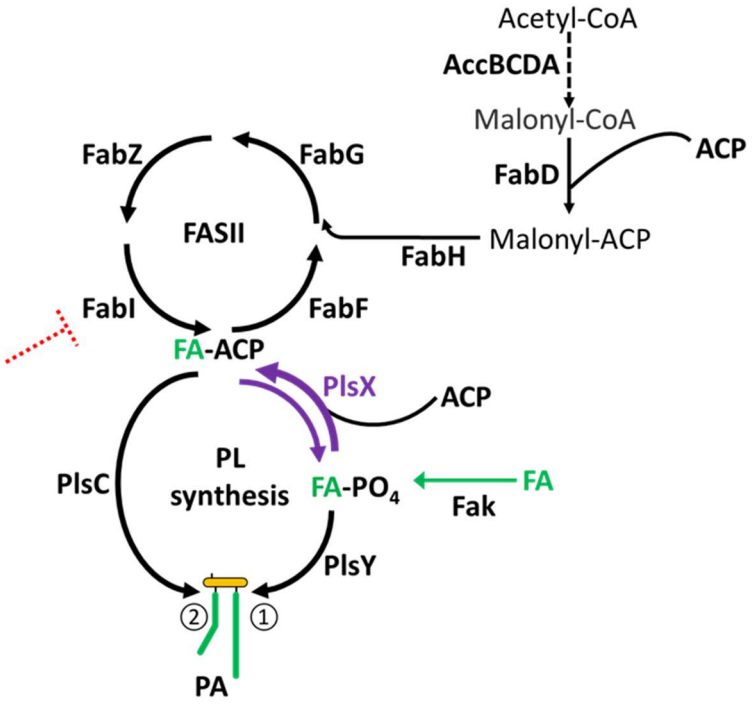

Fig. 1: Roles of the reversible PlsX enzyme in phospholipid synthesis. PlsX (purple) uses the FASII product, acyl-ACP (FA-ACP), as a substrate to produce FA-PO_4, which in turn is used by PlsY to join the acyl group to a glycerophosphate backbone in position 1 (①, bottom). The product, lysophosphatidic acid, is a substrate for PlsC, which then adds the acyl moiety from FA-ACP to position 2 of lyso-PA (②), generating phosphatidic acid (PA). Reverse PlsX activity uses phosphorylated exogenous FAs (green) produced by the fatty acid kinase Fak, to produce FA-ACP. Upon addition of a FASII inhibitor (dashed red T), FAs converted to FA-PO_4 can be used i- as a substrate for PlsY, and ii- as a substrate for reverse PlsX activity, to produce PA. FASII remains active in a Δ*plsX* mutant, but exogenous FAs charged on position 1 and FASII-produced endogenous FAs charged on position 2 for PA synthesis are disconnected. See (1, 6, 9, 11) for references.

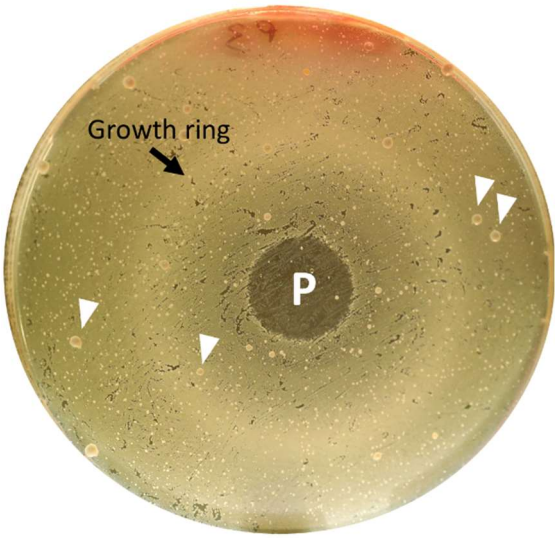

Fig. 2. The FabF inhibitor platensimycin suppresses the Δ*plsX* mutant. Lawns of the Δ*plsX* RN-R derivative prepared on BHI medium lacking supplements were spotted with platensimycin (P, 1.5 µg), incubated 96 h at 37°C, and photographed. The Δ*plsX* mutant is a FA auxotroph. White arrowheads, examples of suppressors. Black arrow, a homogenous growth ring surrounds the platensimycin spot. N=4.

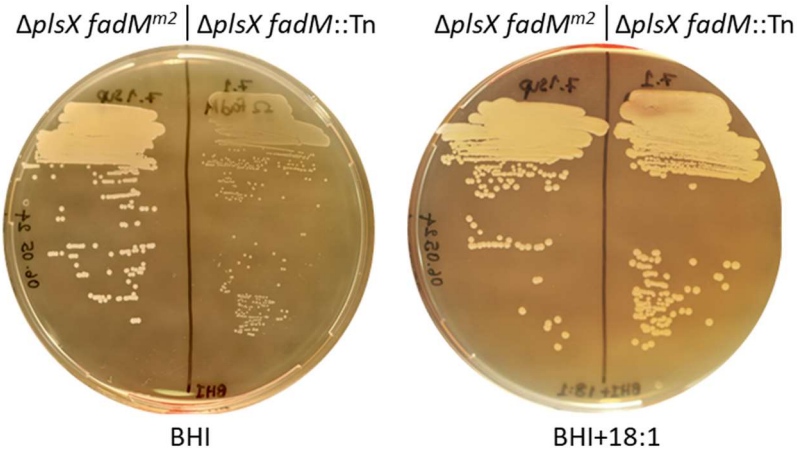

Fig. 3. *fadM* insertional inactivation reverses the *fadM* suppressor phenotype. A *fadM* transposon insertion (24) was transduced into the JE2 Δ*plsX fadM*^{m2} suppressor strain 7.1, giving Δ*plsX fadM*::Tn (**Table S3**). Growth of Δ*plsX fadM*^{m2} and the Δ*plsX fadM*::Tn derivative were compared on solid BHI medium supplemented or not with C18:1. Plates were photographed after 48 h growth at 37°C. Equivalent results were obtained on 3 independent colonies.

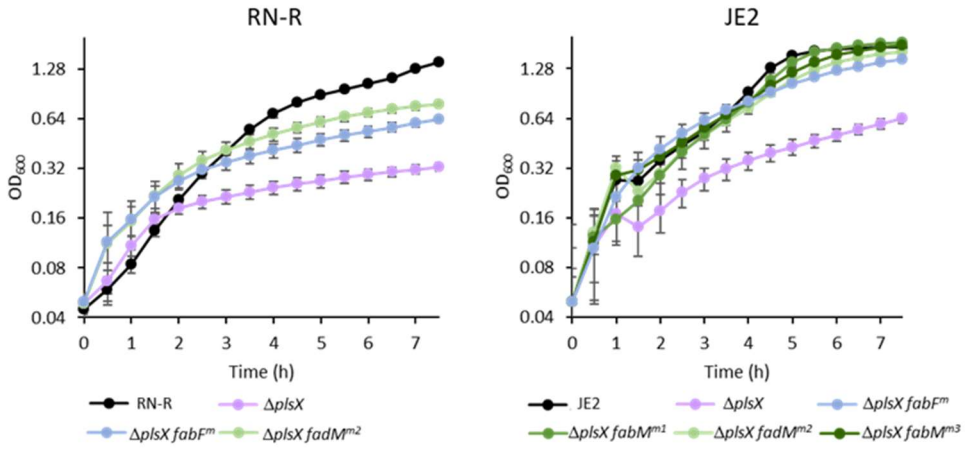

Fig. 4. **Growth in non-FA-supplemented BHI medium of *S. aureus* WT, Δ*plsX* and Δ*plsX fabF* or Δ*plsX fadM* suppressors in RN-R and JE2 backgrounds. Left:** Growth curves of RN-R WT, and derivatives: Δ*plsX*, and Δ*plsX* suppressors encoding FabF^{A119E} or FadM^{Y90F} mutations (*fabF^{m}* and *fadM^{m2}* respectively). **Right:** Growth curves of JE2 WT, and derivatives: Δ*plsX*, and Δ*plsX* suppressors encoding FabF^{A119E}, FadM^{I38T}, FadM^{Y90F}, and FadM^{Y133F} mutations (*fabF^{m}*, *fadM^{m1}*, *fadM^{m2}*, and *fadM^{m3}*, respectively). Growth curves performed on a plate reader show the mean and standard deviation of independent triplicate cultures.

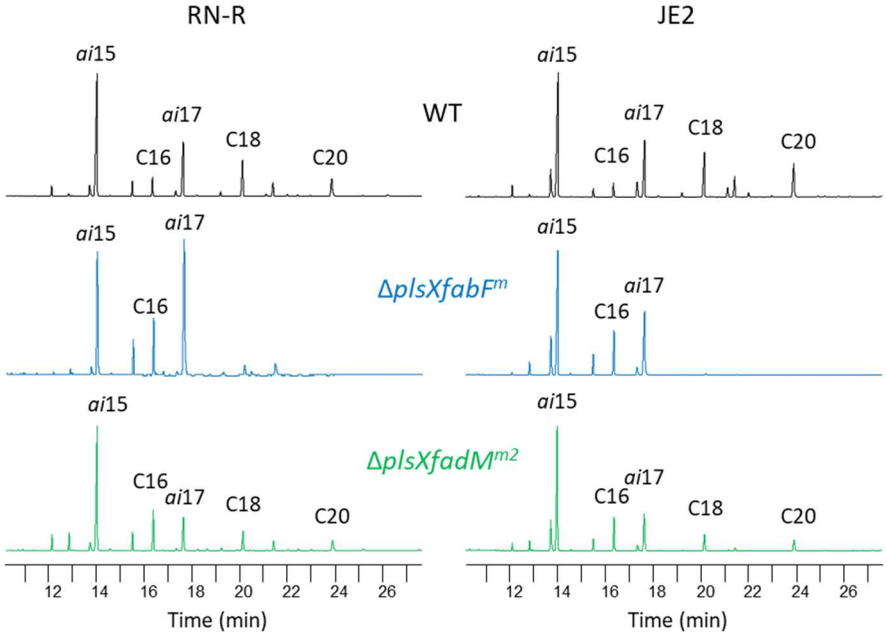

Fig. 5. FA profiles of Δ*plsX* suppressors in RN-R (left column) and JE2 (right column) grown in BHI medium. Suppressors and FA assignments are indicated. *ai*, anteiso; all even numbered FAs are saturated (e.g., C16 is C16:0). The main FA component of WT *S. aureus* is *ai*15 (7). FA lengths in both suppressors, especially in the *fabF* suppressor, are globally shorter than those in the WT parental strain. Peak heights correspond to relative responses (mV) for each sample. Representative of 3 independent determinations giving equivalent results.

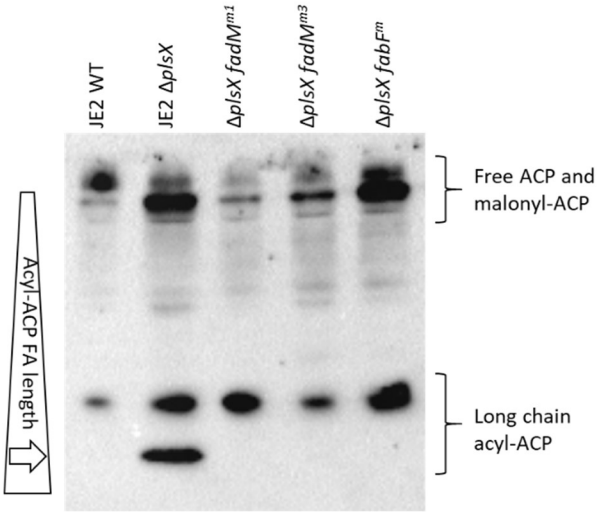

Fig. 6. ACP species in *S. aureus* JE2, Δ*plsX*, and Δ*plsX* suppressor strains. JE2 WT, Δ*plsX fadM*^{m1}, Δ*plsX fadM*^{m3}, and Δ*plsX fabF*^{m} corresponding to strains 7.5, 8.7, and 7.7, respectively (**Table S1**) were grown in BHI. The Δ*plsX* strain was first grown in BHI+C18:1 medium, and then shifted 2h to BHI prior to harvesting. Protein extracts of above strains were loaded on non-denaturing acrylamide gels. Immunoblotting was performed using anti-ACP (7). Acyl-ACP species migration depends on acyl moiety properties (30). As reported, Δ*plsX* accumulates acyl-ACP (left arrow) produced by FASII (5), which cannot be used by PlsC as its substrate, lysophosphatidic acid, is not produced (**Fig. 1**). The intermediate is not detected in WT and Δ*plsX* suppressor strains. The immunoblot is representative of biological duplicates.

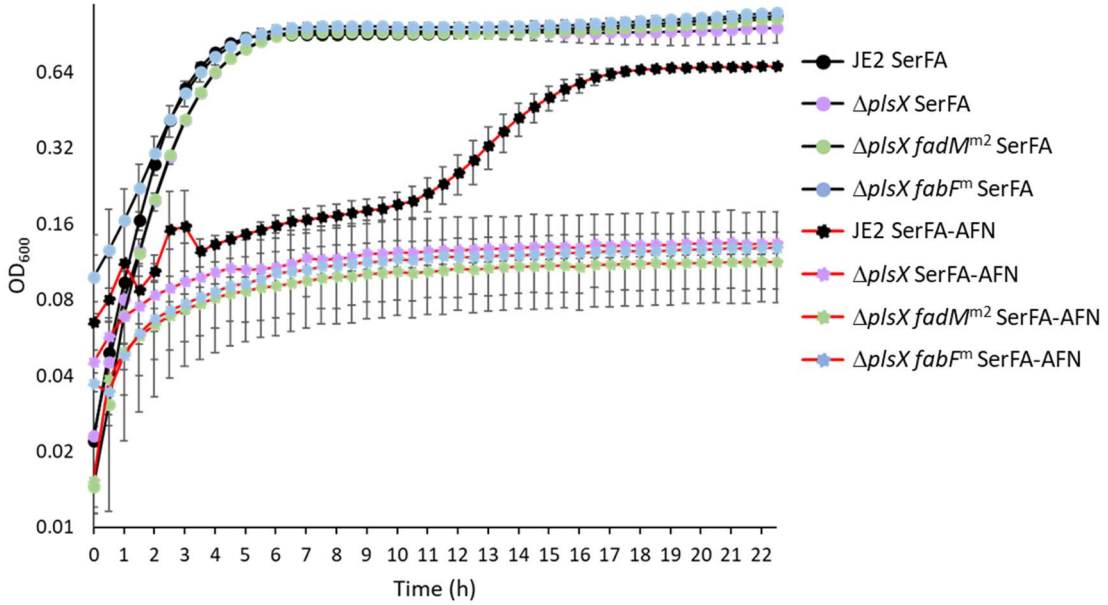

Fig. 7. Effects of anti-FASII treatment on JE2 Δ*plsX*, and Δ*plsX* suppressor strains in FA-supplemented medium. Strains were precultured in SerFA, and grown in SerFA without or with addition of 0.5 µg/ml anti-FASII AFN-1252 (SerFA-AFN). In the presence of AFN, WT *S. aureus* strains incorporate FAs to constitute membrane phospholipids, thus bypassing inhibition. As Δ*plsX* and its suppressors cannot catalyze the reverse reaction needed for FASII bypass (6, 9, 11), they remain sensitive to anti-FASII. Shown are the means and standard deviations of biological triplicate determinations. Experiments were performed on a plate reader. Black lines, no anti-FASII, red lines with anti-FASII. *fadM*^{m2} encodes FadM^{Y90F}; *fabF*^{m} encodes FabF^{A119E}.

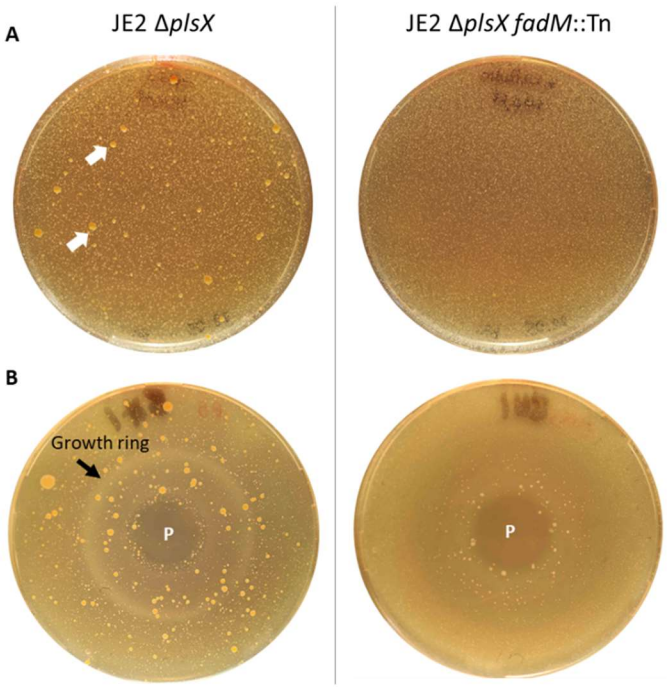

Fig. 8. FabF suppressor mutations do not arise in a Δ*plsX* mutant lacking *fadM*. JE2-derived Δ*plsX* (left) and Δ*plsX fadM*::Tn (derived from strain 7.1: **Table S1**) were plated on BHI solid medium (100 µl of OD_{600} = 0.005) and incubated for 6 days at 37°C, and then photographed. **A**, plates without antibiotics. White arrows point to Δ*plsX* suppressor clones. **B**, platensimycin (P; 1.5 µg) was deposited on plates. Black arrow indicates the growth ring surrounding platensimycin spotting. Results are representative of 2 (**A**) and 3 (**B**) independent cultures.

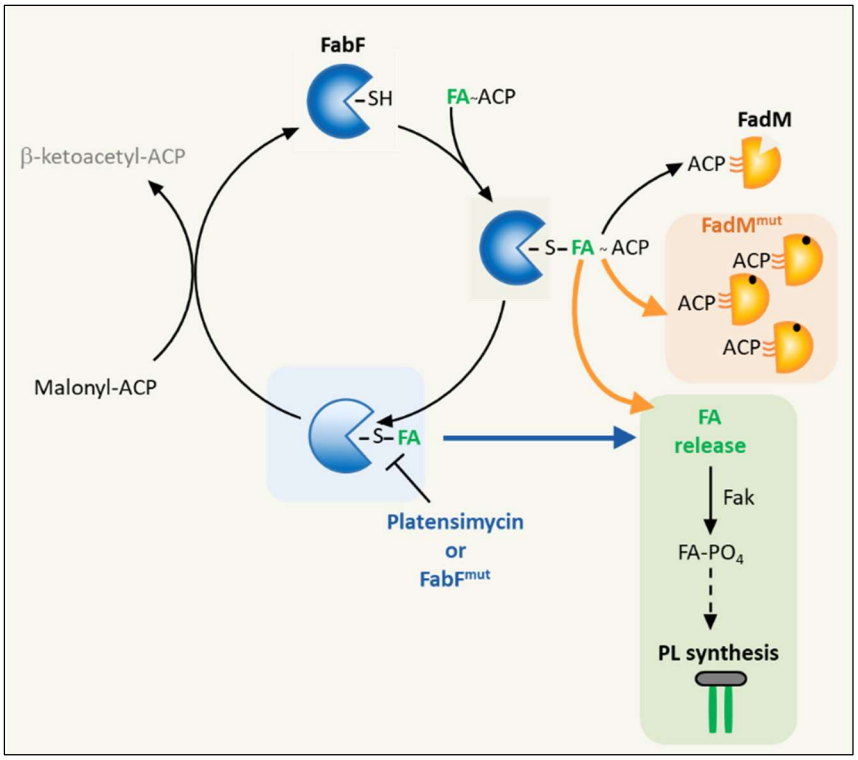

Fig. 9. Model for FabF or FadM mutant coordinated suppression of Δ*plsX* growth arrest. FabF (blue packman) catalyzes the first recursive step of FASII elongation by a ping-pong reaction: it first cleaves its acyl-ACP substrate (FA-ACP), releasing ACP (ping reaction) and allowing malonyl-ACP entry into the FabF cavity, resulting in a 2-carbon addition to the acyl intermediate (pong reaction) (16, 32). The FabF product, β-ketoacetyl-ACP (grey) is the substrate for the next FASII enzyme. We propose that the $FabF^{A119E}$ mutant, or addition of anti-FabF inhibitor platensimycin prevents malonyl-CoA entry, leading to FA release (blue box and arrow). FadM is bifunctional, with acyl-CoA thioesterase and ACP binding activities (17, 19-21). We propose that suppressor mutations in FadM disable its thioesterase activity (black dot in $FadM^{m}$), thus increasing FadM availability for FadM-ACP binding (gold box and arrows). Greater FadM-ACP binding would drive ACP release from the FabF pocket and favor FA leakage. Either of the FabF or FadM mutations would favor release of FAs, to then be phosphorylated by FakA kinase for phospholipid (PL) synthesis (green box). In bold, key effectors of this model. Symbols for FabF are based on (41).

Supplementary Figures and Tables

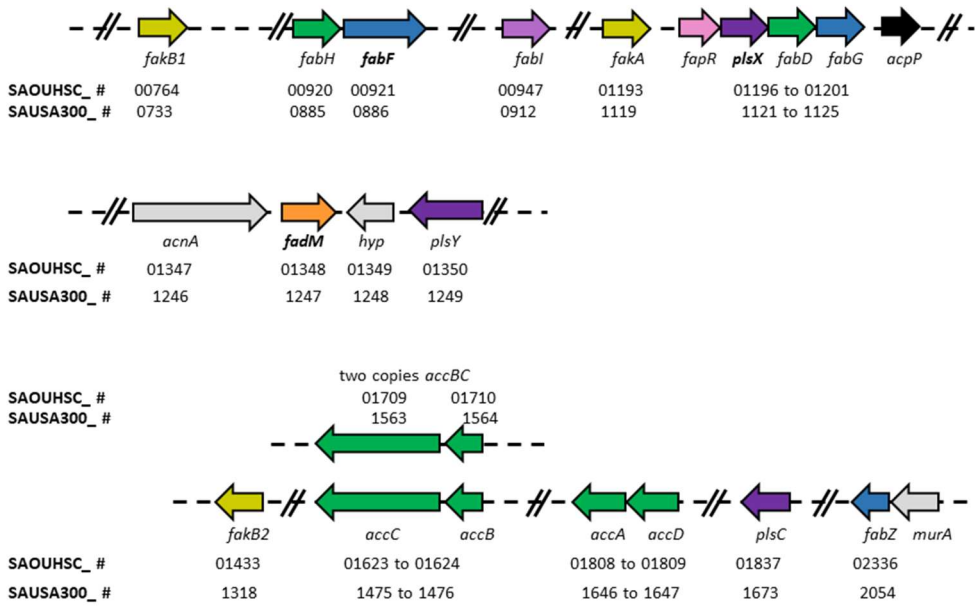

Fig. S1. FASII and phospholipid gene organization in RN-R and JE2 strains. *Orfs* related to this study are in bold. Dark green, FASII initiation; blue, FASII elongation; black, acyl carrier protein (*acpP*); purple, phospholipid synthesis; olive, FASII bypass fatty acid kinase; pink, regulatory; orange, FadM; grey, not directly related. Locus names are given for USA300 FPR_3797 (JE2) and 8325-4 (RN-R parent).

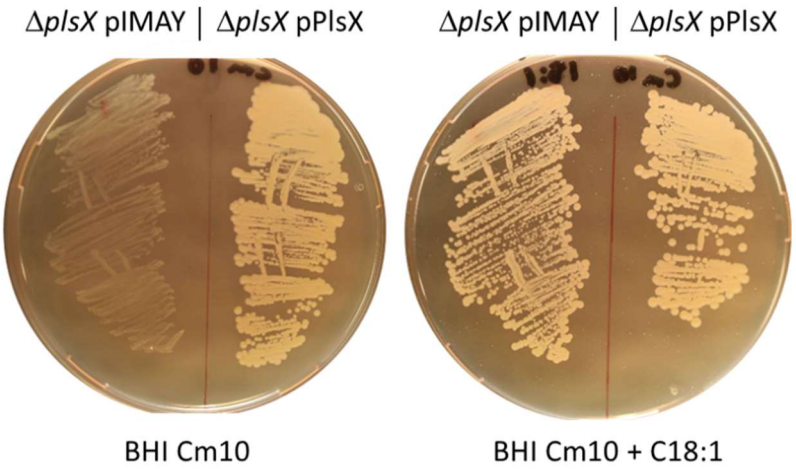

Fig. S2. Complementation of Δ*plsX* by a plasmid-carried *plsX* gene. RN-R Δ*plsX* strains containing an empty plasmid (pIMAY; left side of plates), or a plasmid carrying the *plsX* orf expressed from its native promoter on pIMAY (pPlsX; right side of plates), were streaked on BHI-chloramphenicol (Cm) 10 µg/ml solid medium without, or with C18:1 (250 µM) to bypass *plsX* absence. Plates were photographed after 48h growth at 30°C. The Δ*plsX* strain carrying the empty plasmid failed to grow in the absence of C18:1 supplementation, while the pPlsX-complemented strain grew in both media.

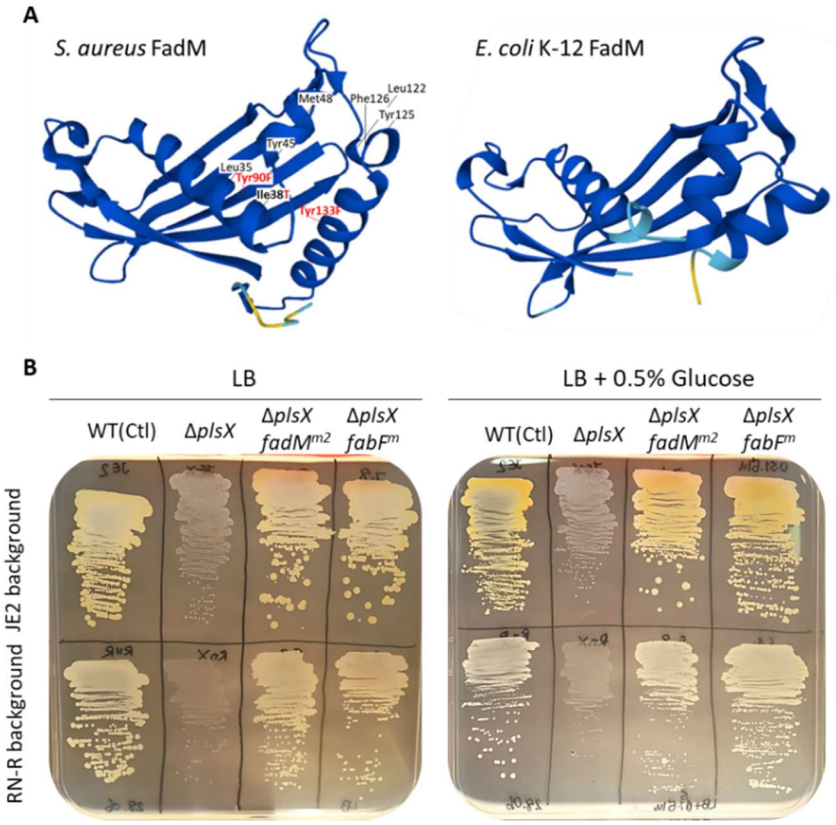

Fig. S3. Evidence that FadM^m suppression of PlsX depletion does not require acyl-CoA thioesterase activity. A. FadM structures in *S. aureus* (left) and *E. coli* (right), as based on protein structures (respective PDBs: 6FDG and INJK), and modelling generated by Alphafold (42, 43). In black, amino acids in the FA-binding cavity of *S. aureus* acyl-CoA thioesterase (17). In red, amino acids altered in *fadM* suppressors of Δ*plsX*; n.b., I38 is in the binding cavity and also mutated. All FadM suppressor mutations localize to the FA-binding cavity. **B.** The FadM^m suppressor phenotype is not subject to glucose repression, suggesting against involvement of Fad-mediated acyl-CoA synthesis. FA degradation (Fad) enzyme FadE converts FA to acyl-CoA, a FadM substrate. The *fad* operon is subject to CcpA-glucose repression (24, 26), suggesting that acyl-CoA pools would drop in glucose-containing medium. Strains precultured in LB and LB with C18:1 for Δ*plsX* (Materials and Methods) were streaked directly on solid LB medium with or without 0.5% glucose. Upper and lower rows, strains are derived from JE2 and from RN-R, respectively. Results represent biological triplicates.

Table S1. Δ*plsX* suppressors [a,b].

	Gene : protein mutations in Δ*plsX* suppressor mutants				
	SAUSA300_0886 FabF (3-oxoacyl-ACP synthase II)		SAUSA300_1247 FadM (acyl-CoA thioesterase/ACP-binding (17, 19-21))		
Strain name	*fabF*^{m}: FabF^{A119E}	*fabF*^{m2}: FabF^{D266A}	*fadM*^{m1}: FadM^{I38T}	*fadM*^{m2}: FadM^{Y90F}	*fadM*^{m3}: FadM^{Y133F}
RN4220 5.1	X		NT	NT	NT
RN4220 5.2	X		NT	NT	NT
RN4220 5.3	X		NT	NT	NT
RN4220 5.4	X		NT	NT	NT
RN4220 5.5	X		NT	NT	NT
RN4220 5.6				X	
RN4220 5.7				**X**	
RN4220 5.8				X	
RN4220 6.1	X		NT	NT	NT
RN4220 6.2	X		NT	NT	NT
RN4220 6.3	X		NT	NT	NT
RN4220 6.4	X		NT	NT	NT
RN4220 6.5	X		NT	NT	NT
RN4220 6.6	X		NT	NT	NT
RN4220 6.7				X	
RN4220 6.8	X		NT	NT	NT
JE2 7.1				**X**	
JE2 7.2			X		
JE2 7.3				X	
JE2 7.4			X		
JE2 7.5			X		
JE2 7.7	X		NT	NT	NT
JE2 7.8	X		NT	NT	NT
JE2 8.1			X		
JE2 8.2				X	
JE2 8.3			X		
JE2 8.4			X		
JE2 8.5			X		
JE2 8.6			X		
JE2 8.7					X
JE2 8.8					X
JE2 Sup1 [b]	X				
JE2 Sup2 [b,c]		X			
JE2 Sup3 [d]					

[a] The red 'X' indicates that the mutation is present in the tested isolate. NT, not tested. Suppressors identified from total genome sequencing are in bold. Strains written in green were chosen for further study. [b] Sup1 and Sup2 suppressors of Δ*plsX* had the same secondary mutation in SAUSA300_100 (generating Csa1A^{K185Q}), which was absent in subsequently isolated suppressors mapping to *fabF*. [c] Sup2, encoding FabF^{D266A}, could not be propagated after storage. [d] Sup3, carrying a mutation in SAUSA300_0150 (encoding a putative transposase with a P71S mutation), was not further studied.

[b] **Accompanying Table S2 is joined as an Excel file.**

Table S3. Genetic materials.

Strains			
Host strain	**Strain**	**Description**	**Reference**
JE2 USA300_FPR3757	JE2 (WT)	USA300_FPR3757 cured of its three native plasmids	(24)
	Δ*plsX*	In-frame *plsX* deletion leaving operon intact	This study
	Δ*plsX* suppressor in *fadM*; *ΔplsXfadM*^{m1}	*fadM*^{m1} encodes FadM^{I38T}	This study
	Δ*plsX* suppressor in *fadM; ΔplsXfadM*^{m2}	*fadM*^{m2} encodes FadM^{Y90F}	This study
	Δ*plsX* suppressor in *fadM; ΔplsXfadM*^{m3}	*fadM*^{m3} encodes FadM^{Y133F}	This study
	Δ*plsX* suppressor in *fabF; ΔplsXfab*^{m}	*fabF*^{m} mutant encodes FabF^{A119E}	This study
	fadM Tn insertion	JE2 derivative containing an erythromycin-resistance-marked transposon (Tn) insertion in SAUSA300_1247 at position 1384915 (based on JE2 genome entry NZ_CP020619)	(24)
	Δ*plsX fadM*::Tn	Φ80 phage transduction of the SAUSA300_1247 Tn insertional mutant into the Δ*plsX fadM*^{m2} (7.1) suppressor	This study
RN-R 4220	RN-R 4220 (WT)	RN4220 derivative repaired for *fakB1*	(14)
	Δ*plsX*	In-frame deletion of *plsX* leaving operon intact	This study
	Δ*plsX* suppressor in *fadM; ΔplsXfadM*^{m2}	*fadM*^{m2} mutant encodes FadM^{Y90F}	This study
	Δ*plsX* suppressor in *fabF; ΔplsXfabF*	*fabF* mutant encodes FabF^{A119E}	This study
Plasmids			
	Plasmid	**Description**	**Reference**
	pMAD	Thermosensitive plasmid used to generate double-crossover deletion events	(35, 36)
	pMAD::*fapR-fabD* fragments	Used to generate *plsX* deletion	This study
	pIMAY	Used for *plsX* cloning	(37, 44)
	pIMAY::*plsX*	Used for *plsX* complementation in Δ*plsX*	This study
Transducing phage			
	Phage	**Description**	**Reference**
	ϕ80	Used to transduce erythromycin-resistance-marked Tn insertion of SAUSA300_1247 into Δ*plsXfadM*^{m2} background	(45)

Table S4. Oligonucleotides (5' to 3') used for genetic constructions and mutant detection.

Construction type and primers used for detection		Description
Plasmid for Δ*plsX* construction on pMAD linearized by SmaI		
pMAD_FapR_F	TCTATCGATGCATGCCATGGTACCCCTTCATCACAGACCATGAACTAAGC	*fapR* fragment
FapR_FabD_R	CGGAAAAATAATTGCTGTTTTACTCATAATTTTATCCTCGCTTATCATAAAAC	
FapR_FabD_F	GTTTTATGATAAGCGAGGATAAAATTATGAGTAAAACAGCAATTATTTTTCCG	*fabD* fragment
FabD_pMAD_R	GCAGAAGCTTCTAGAATTCGAGCTCCCTGTGACCTGAAACAACAATTTGACC	
Verifications for pMAD constructions		
pMAD_F	GTTACGTTACACATTAACTAGACAG	
pMAD_R	TGGACAGCATGGCCTGCAACGC	
Cloning *plsX* on pIMAY-derived locus1 plasmid		
pIMAY_FapR_F	AGTTTGTGGTTTAATGGGGTTGACACTTGAACTATTTAAA	*fapR* fragment
FapR_PlsX_R	TCAATTGCTAATTTAACCATTTTTTAGTACCTAGTCTTAA	
FapR_PlsX_F	TTAAGACTAGGTACTAAAAAATGGTTAAATTAGCAATTGA	*plsX* fragment
plsX_pIMAY_R	TTGTTGCTATAATGAAATGCGTTCTTACTCATTTGATTCACCTA	
pIMAY_FapR_R	TTTAAATAGTTCAAGTGTCAACCCCATTAAACCACAAACT	pIMAY linearized by reverse PCR
plsX_pIMAY_F	TAGGTGAATCAAATGAGTAAGAACGCATTTCATTATAGCAACAA	
Δ*plsX* suppressor verifications		
FabF_F	GGAATCAGCTAGAGAACGC	SAUSA300_0886
FabF_R	CATTTTTCAACCCACAAGAGG	
1247_F	AATCGGTATTTGAGGCAC	SAUSA300_1247
1247_R	ATCTTCACGCTAATTACATT	
0100_F	CGTGGCCTGGATATGATGAT	SAUSA300_0100 *csa1*
0100_R	GATTATCCTGAGCTACTTCG	
0150_F	TTGGCAGTAATTGACTGAAC	SAUSA300_0150 pseudogene
0150_R	GGTCCTTGTCGATACCTATCA	
Verifications of Tn insertion in SAUSA300_1247		
1247_F	GGATTACTATCGTCACGGTGG	Transposon insertion
UpBursa_F	CTCGATTCTATTAACAAGGG	